Mater. Res. Soc. Symp. Proc. Vol. 1124 © 2009 Materials Research Society 1124-Q07-09

Temporal Evolution of the Concrete-Bentonite System Under Repository Conditions

Elena Torres, Alicia Escribano, María J. Turrero, Pedro L. Martin, Javier Peña, María V. Villar
Division of Engineered and Geological Barriers, CIEMAT, Avda. Complutense 22, 28040,
Madrid, Spain

ABSTRACT

Concrete could be part of the barrier system and/or be needed during repository construction for the management of the High Level Radioactive Waste (HLW) in a Deep Geological Repository (DGR). Depending upon the design, concrete could be physically in contact with the bentonite, or be sufficiently close that alkaline pore fluid from the cement may interact with the bentonite, affecting its properties. A comprehensive study based on a series of short term experiments is being performed to provide experimental evidences on the physical, chemical and mineralogical changes during the concrete-compacted bentonite interaction. Concrete and bentonite samples were analyzed by means of XRD, FTIR spectroscopy and SEM-EDS. In addition, in bentonite sections, swelling capacity measurements, specific surface area (BET) and chemical analysis for cation exchange capacity and soluble salts were performed.

INTRODUCTION

A Deep Geological Repository (DGR), based on the concept of multibarriers, is the solution proposed by most countries for the management of High Level Radioactive Waste (HLW). In order to isolate the wastes, a series of barriers are inserted between the wastes and the biosphere.

The Spanish repository design contains concrete to support the access galleries and in the final sealing of access routes. Concrete will be in contact with the geological clay formation and the bentonite barriers. Cement in contact with the bentonite barrier will be a source of alkaline fluids in wet conditions. Concrete pore fluids are in quasi-equilibrium with the solid hydrated phases of the matrix [1]. Ca solubility is principally controlled by $Ca(OH)_2$. Sulphate solubility is limited by ettringite. The Mg contents are controlled by $Mg(OH)_2$ and Al solubility by C_3AH_6. Si concentrations are determined by the solubility of alkali-containing C-S-H gels. Alkaline cement pore water enhances the solubility of many radioactive elements.

Furthermore, concrete degradation generates a diffusive alkaline plume which can affect the swelling and transport properties of the bentonite, as well as the properties of the adjacent host rock and groundwater. Many studies have been performed in order to study the influence of alkaline media on bentonite. Eberl et al. [2] reported that the formation of illite or illite/smectite depends on the solution concentration rather than on temperature and time of reaction.

Cuevas et al. [3] have carried out a set of batch (alkaline solution and bentonite, 25-200ºC) and column experiments (granitic and alkaline water-mortar-bentonite, 25-120ºC) experiments in order to study the influence of alkaline media on FEBEX bentonite. The main phases identified in the alkaline reaction of FEBEX bentonite are phillipsite, Mg-clays, analcime, tobermorite and C-S-H gels. The formation of a new smectitic trioctahedral phase was confirmed, as well.

The scope of the present study is to provide experimental data about alteration products at the concrete/bentonite interface and the related changes of the bentonite and concrete properties under these conditions.

EXPERIMENTAL

Materials

The tests were performed with the Spanish reference bentonite (FEBEX bentonite) from the Cortijo de Archidona deposit (Almería, Spain). FEBEX bentonite[4] has a content of dioctahedral smectite of the montmorillonite type of 92±3%. It contains variable quantities of quartz (2±1%), plagioclase, cristobalite (2±1%), potassium feldspar (traces), calcite (traces) and trydimite (traces). The cation exchange capacity is 102 meq/100 g, and the exchangeable cations are Ca (35±3 meq/100g), Mg (31±3 meq/100g), Na (27.1±0.2 meq/100g) and K (2.6±0.4 meq/100g). The cement used in the tests is a Sulfate-Resistant Portland Cement CEM I 42.5 R/SR [5]: its chemical composition is shown in Table I.

Table I. Chemical composition of the CEM I 42.5 R/SR cement.

CHEMICAL COMPOSITION (WT. %)	**SIO_2**	**AL_2O_3**	**FE_2O_3**	**CAO(TOTAL)**	**MGO**	**SO_3**	**NA_2O**	**K_2O**	**CAO(FREE)**
	19.6	4.43	4.27	64.5	0.95	3.29	0.11	0.28	1.92

Experimental Set up

The tests were carried out in hermetic cylindrical cells in which a concrete slab was placed on the top of the compacted bentonite block. For hydration, a saline solution, whose composition is described in Table II, was used. The hydration solution is injected under a pressure of 12 bars. A plane heater constitutes the bottom of the cell and on the top of the cell a chamber allows the circulation of water at a controlled temperature (around 22ºC), lower than that of the heater (100ºC), so a gradient of temperature is established. A hydration channel crosses the upper chamber and allows the hydration of the sample through a stainless steel sinter. The body of the cell is made out of Teflon, although an external steel cylinder prevents its deformation swelling. The clay, with its water content at equilibrium with the laboratory conditions, is uniaxially compacted outside the cell to a dry density of 1.65 g/cm^3. The cells are inside a methacrylate chamber, under vacuum, to prevent oxidation. Six medium cells were assembled. In the context of NF-PRO project, three cells were dismantled after 6, 12 and 18 months. The remaining cells are planned to operate for at least two years more. Two sensors were installed in each cell to monitor the evolution of water content and temperature with time. Sensors were located 50 and 95 mm from the top of the cell, at the hydration zone and the interface, respectively.

Table II. Chemical composition of the saline solution.

Na(M)	**Ca(M)**	**Mg (M)**	**SO_4^{2-} (M)**	**Cl^-(M)**	**HCO_3^-(M)**	**pH** = 7.54 **pE** = -3.16 **log P CO_2** = -2.65
1.3 E-01	1.1 E-02	8.2 E-02	7.0 E-02	2.3 E-02	1.8 E-03	

Methods

Three types of samples were analyzed: (1) the precipitates found at the concrete/bentonite interface and some millimetres far away from interface; (2) bentonite samples at different distances from the interface, named sections 1, 2 and 3; and (3) concrete sections representative of the whole slab. The samples collected were analyzed by using different techniques: X-ray diffraction (XRD) [Philips Xpert-MPD diffractometer], Fourier transform-infrared spectroscopy (FT-IR) [Nicolet 4700 in the range of 4000 to 400 cm^{-1}], Scanning Electron Microscopy (SEM) with microanalysis (XEDS) [JEOL JSM 6400], and N_2-BET specific surface area methods. Cation exchange capacity (Cu-triethylenetetramine method) [6], and exchangeable cations ($CsNO_3$ method) [7] analysis were also performed.

RESULTS

Concrete degradation

Carbonation represents the main degradation process observed in the concrete slabs from the dismantled cells. Calcite precipitates in the hydration zone to a greater extend than in the rest of the slab and increases with time (Figure 1). Leaching of the most soluble elements, such as alkali hydroxides, leads to the reprecipitation of portlandite (Figure 2) and brucite on the bottom part of the concrete blocks. The effects of temperature, humidity and hydration with a solution rich in sulphates favour the formation of ettringite [$Ca_6Al_2(SO_4)_3(OH)_{12}\,26(H_2O)$] and gypsum ($CaSO_4{\cdot}H_2O$). Ettringite was found in the 12-month test (Figure 3). In concrete tested for 18 months, together with ettingite, gypsum was also formed (Figure 4), possibly resulting from the substitution reaction between portlandite and sulfate, either from the saline solution or from the dissolution of initial gypsum. Although gypsum is a common component of Portland cement, the amount measured, by means of XRD and TGA analysis, in the 18-month reacted concrete was much greater than the average content of gypsum found in the unaltered sample.

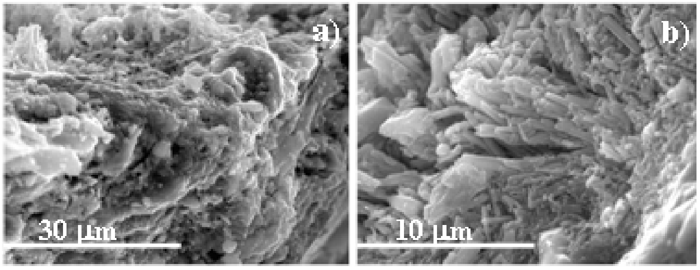

Figure 1. Calcite: (a) in the hydration zone of the cell after 6 months and (b) inside of a pore after 12 months.

Concrete/bentonite interface

A continuous layer of portlandite was found in the three cells (Figure 5a). According to the EDS line profile, in the 18 months test, the layer is 2 μm thick (Figure 5b and 5c). Portlandite formation is a consequence of the previous leaching of the matrix concrete by diluted groundwaters providing pore water oversaturated with respect to portlandite.

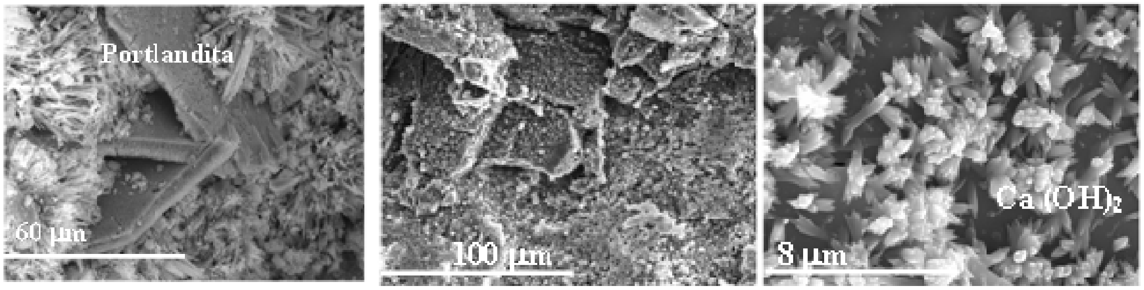

Figure 2. Portlandite: (a) inside of a pore after 6 months, (b) covering the sample surface after 12 months, and (c) detail of the crystals.

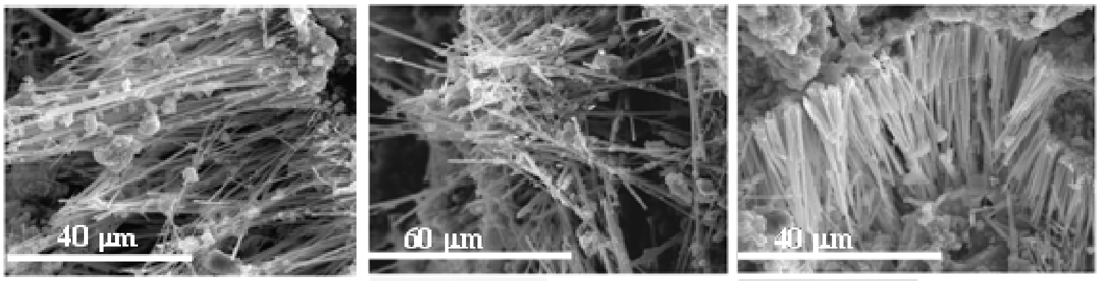

Figure 3. Ettringite: in a cell dismantled after 12 months.

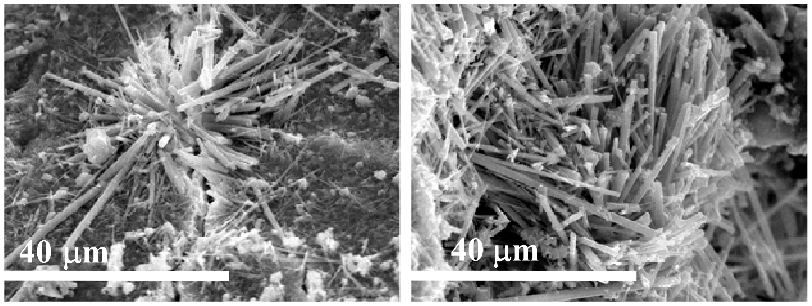

Figure 4. Gypsum crystals after 18 months.

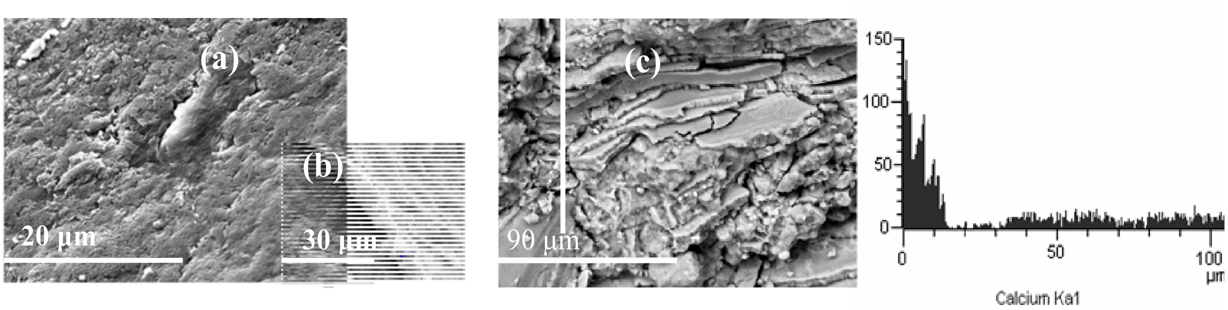

Figure 5. (a) Portlandite precipitate layer on the bentonite surface from the 18 month test. (b) Thickness of the precipitate layer. (c) Bentonite interface profile and variation of the Ca concentration (cps) from interface.

Below the portlandite layer, CSH gels were formed. Tobermorite-type phases (Ca/Si molar ratio of 0.6), were identified together with brucite and ettringite (Figure 6). Also, in the 18-month test, marks of dissolution of quartz were detected. This process enables the precipitation of CSH minerals such as tobermorite.

X-ray diffraction confirmed the formation of a smectitic trioctahedral phase. The peak found at 1.53 Å is typical of saponite (Figure 7a). In the FTIR spectrum of the sample collected at the interface, a small band was observed at 669 cm^{-1}. This band could correspond to the Mg_3OH bending vibration of saponite. XRD analysis of the oriented aggregates of the fraction below 2 μm shows an increase of the d-spacing. The increase of the interlayer space in the smectite could result from the formation of a brucite-saponite-smectite mixed phase. This process does not depend on time, as it can be observed in figure 7b.

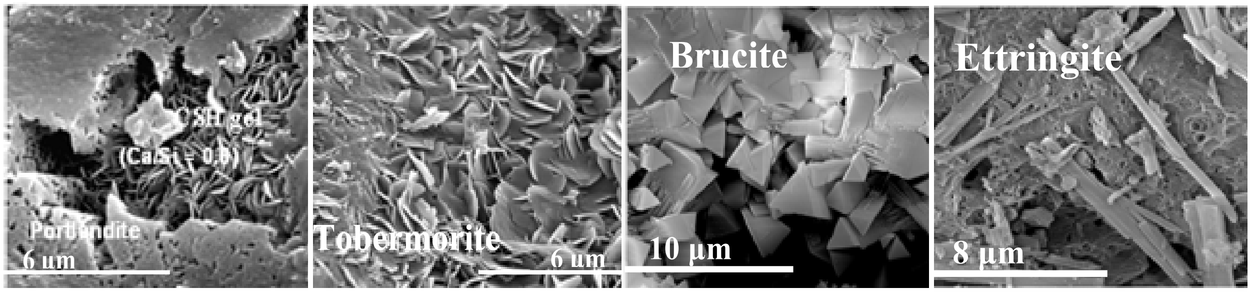

Figure 6. New phases formed at the concrete-bentonite interface.

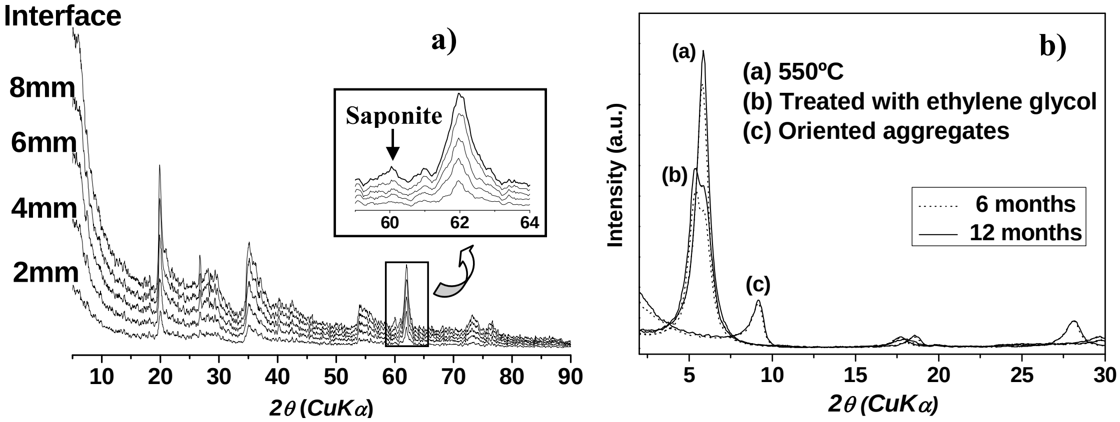

Figure 7. (a) XRD patterns of the bentonite at different depths in the 18 month test, (b) XRD diffraction profile of the oriented aggregates.

Bentonite

Regarding exchangeable cations (Figure 8), Ca^{2+} and K^+ do not manifest consistent variations along of the compacted bentonite block. Nevertheless, an increase of Na^+ and a drop in Mg^{2+} is observed at the interface. At the interface, Mg^{2+} is released from exchangeable positions and is introduced into octahedral sites. Because of this Mg^{2+} mobility, saponite can be formed.

Cation Exchange Capacity (CEC) in bentonite tends to rise as we approach the interface. As a result of CSH precipitation, there is a marked increase in the CEC values.

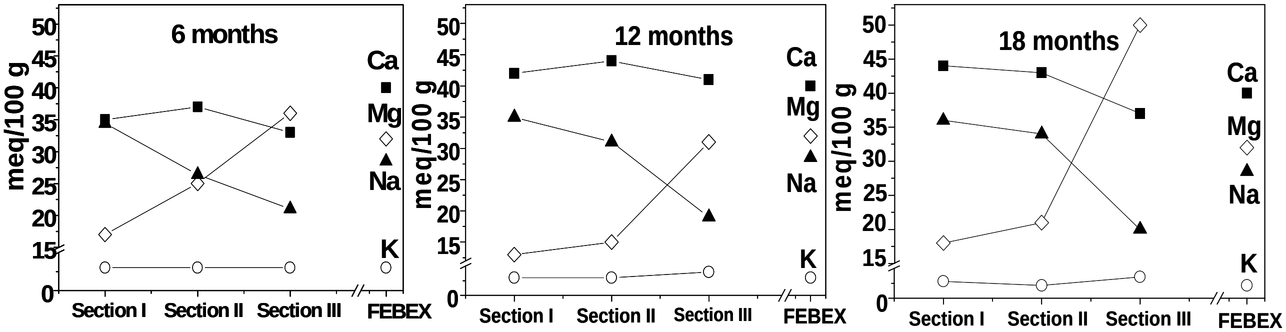

Figure 8. Distribution of the exchangeable cations in bentonite in the different experiments (from the interface, section 1: 3 to 25 mm; section 2: 25 to 50 mm; section 3: 50 to 78 mm).

The temperature gradient induces the movement of soluble salts towards the heater. Cl^-, SO_4^{2-} and Na^+ increase in the bentonite section closer to the heater.

CONCLUSIONS

Due to hydration in the cells, the leaching of salts contained in the porous and soluble concrete compounds induces the precipitation of new mineral phases at the interface of both materials. The secondary mineral phases formed are: CSH-gel tobermorite-type (Ca/Si = 0.6), portlandite, brucite and ettringite. The interlayer space in the smectite at the interface corresponds to a brucite-saponite-smectite mixture phase. Chloride, sulfate and sodium contents increase near the heater, resulting in the precipitation of NaCl near the heater.

Mineralogical and chemical changes were observed in the bentonite in contact with concrete. CEC values increase because of the formation of calcium silicate hydrate gel. A significant variation in the magnesium content and sodium at the exchange positions was measured.

ACKNOWLEDGEMENTS

This work has been financially supported by ENRESA and the EU NF-PRO project under contract FIGW-CT-2003-02389.

REFERENCES

1 M. García-Gutiérrez, U. Alonso, T. Missana, M. Mingarro, N. Granizo, M. Grivé, X. Gaona, E. Colás, L. Duro and J. Bruno, *Estudio bibliográfico sobre sorción y difusión de radionucleidos en cementos, hormigones y productos de corrosión en presencia de cementos*, Report PT-02/2007, (ENRESA, Madrid, 2007).
2 D.D. Eberl, B. Velde and T. McCormick, *Clay Miner.* **28**, 49 (1993).
3 J. Cuevas, R. Vigil de la Villa, S. Ramírez, L. Sánchez, R. Fernández, and S. Leguey, *J. of Iberian Geology* **32**, 151 (2006).
4 A.M. Fernández, B. Baeyens, M. Bradbury and P. Rivas, *Phys. Chem. Earth, Parts A/B/C*, **29(1)**, 105 (2004).
5 A. Hidalgo, S. Petit, C. Domingo, C. Alonso, C. Andrade. *Cem. Concr. Res.* **37**, 67 (2007).
6 L.P. Meier and G. Kahr, *Clays and Clay Miner.* **47(3)**, 386-388 (1999).
7 B.L. Shawhney. *Clays and Clay Miner.* **18**, 47 (1970).